

Relativistic high-harmonic generation and correlated electron acceleration from plasma mirrors at 1 kHz repetition rate

S Haessler, F Böhle, M Bocoum, M Ouillé, J Kaur, D Levy, L Daniault, A Vernier, J Faure, R Lopez-Martens

▶ **To cite this version:**

S Haessler, F Böhle, M Bocoum, M Ouillé, J Kaur, et al.. Relativistic high-harmonic generation and correlated electron acceleration from plasma mirrors at 1 kHz repetition rate. 2020. hal-02991825

HAL Id: hal-02991825
https://hal.science/hal-02991825

Preprint submitted on 6 Nov 2020

HAL is a multi-disciplinary open access archive for the deposit and dissemination of scientific research documents, whether they are published or not. The documents may come from teaching and research institutions in France or abroad, or from public or private research centers.

L'archive ouverte pluridisciplinaire **HAL**, est destinée au dépôt et à la diffusion de documents scientifiques de niveau recherche, publiés ou non, émanant des établissements d'enseignement et de recherche français ou étrangers, des laboratoires publics ou privés.

arXiv:2005.01343v1 [physics.plasm-ph] 4 May 2020

Relativistic high-harmonic generation and correlated electron acceleration from plasma mirrors at 1 kHz repetition rate

S. Haessler,[1,*] F. Böhle,[1] M. Bocoum,[1] M. Ouillé,[1,2] J. Kaur,[1] D. Levy,[3] L. Daniault,[1] A. Vernier,[1] J. Faure,[1] and R. Lopez-Martens[1]

[1] *Laboratoire d'Optique Appliquée, CNRS, Ecole Polytechnique, ENSTA Paris, Institut Polytechnique de Paris, 181 chemin de la Hunière et des Joncherettes, 91120 Palaiseau, France*

[2] *Ardop Engineering, Cité de la Photonique, 11 Avenue de la Canteranne, bât. Pléione, 33600 Pessac, France*

[3] *Department of Physics of Complex Systems, Weizmann Institute of Science, Rehovot 7610001, Israel*

We report evidence for the first generation of XUV spectra from relativistic surface high-harmonic generation (SHHG) on plasma mirrors at a kilohertz repetition rate, emitted simultaneously and correlated to the emission of energetic electrons. We present measurements of SHHG spectra and electron angular distributions as a function of the experimentally controlled plasma density gradient scale length Ł for three increasingly short and intense driving pulses: 24 fs (9 optical cycles) and $a_0 = 1.1$, 9 fs (3.5 optical cycles) and $a_0 = 1.8$, and finally 4 fs (1.7 optical cycles) and $a_0 \approx 2.0$. For all driver pulses, we observe relativistic SHHG in the range Ł $\in [\lambda/25, \lambda/10]$, with an optimum gradient scale length of Ł $\approx \lambda/15$.

Surface high-harmonic generation (SHHG) [1] from relativistic plasma mirrors is a promising method for greatly enhancing the available energy of attosecond XUV pulses. This is motivated by the absence of an inherent limitation for the driving intensity such that extremely large numbers of photons from ultra-high intensity lasers can can be converted into attosecond XUV pulses. In strongly relativistic conditions with a normalized vector potential $a_0 = \sqrt{I[\mathrm{W\,cm^{-2}}]\,\lambda_0^2[\mu\mathrm{m}^2]/(1.37\times10^{18})} \gg 1$, where I is the laser intensity and λ_0 the central wavelength, this is expected to occur with extremely high, percent-level conversion efficiencies [2–4]. Reported experimentally observed laser-to-XUV conversion efficiencies for plasma mirrors with $a_0 \sim 1$ are $\sim 10^{-4}$ [5–8], but are expected to increase with higher-intensity drivers.

Reaching relativistic SHHG regime with $a_0 > 1$ requires an on-target intensity of $\gtrsim 10^{18}\,\mathrm{W/cm^2}$ for an 800-nm laser while retaining a very steep surface plasma density profile, i.e. a profile $n(x) = n_\mathrm{c}\exp[x/Ł]$, with a scale length Ł of a small fraction of the diving laser wavelength. Here n_c is the nonrelativstic critical plasma density for the driving wavelength and x is the coordinate in the target normal direction. Technically this requires a highly focusable terawatt-class driver laser with a temporal contrast of $\gtrsim 10^{10}$. These conditions are typically met by Joule-class amplifier chains with dedicated contrast filters [9, 10] and operating at $\sim 10\,\mathrm{Hz}$ repetition rate [4–9].

Many applications as well as parametric studies of this regime would benefit from a higher repetition rate. At LOA, we have developed a unique laser chain with power-scaled hollow-core-fiber postcompression system [11] operating at 1 kHz repetition rate. Using this kHz-laser, which achieves ultra-high intensties with few-mJ pulse energy and few-cycle pulse duration, we have demonstrated laser-plasma interaction in the relativistic regime through laser-wakefield acceleration of electrons both in underdense gas jets [11, 12] and in the underdense part of a smooth plasma density gradient on a plasma mirror [13]. Here we report on the first experimental demonstration of relativistic SHHG at kHz-repetition rate, the arguably most demanding application in terms of laser performance as it depends critically on the spatio-temporal pulse quality and the temporal contrast.

For relativistic driving intensities, $a_0 \gtrsim 1$, the SHHG emission mechanism is described by a push–pull process [14], also dubbed "relativistic electron spring" [15, 16], repeating once per driving laser period. The incident laser field first pushes electrons into the plasma, piling up a dense electron bunch and creating a restoring internal plasma field. As the laser field changes sign, the combined plasma and laser fields accelerate the electron bunch to a relativistic velocity towards the vacuum. SHHG

* stefan.haessler@ensta-paris.fr

emission then either results from a pure phase modulation of the incident laser field by the relativistically moving critical-density plasma surface ["relativistic oscillating mirror" (ROM)] [2, 17, 18], or as a coherent synchrontron emission (CSE) from the relativistically moving dense electron bunch as it gets accelerated orthogonally by the laser electric field [3, 19, 20].

For $a_0 \sim 1$, this relativistic SHHG emission needs to be discriminated from coherent wake emission (CWE) [1, 21], generated already at sub-relativsitic intensities, $a_0 < 1$. Once per laser field cycle, Brunel electrons [22] are accelerated out and back into the surface plasma to form, via collective trajectory crossings, a spatially localized electron density peak. This peak traverses the overdense part ($n(x) > n_c$) of the plasma density gradient and in its wake excites plasma oscillations at the local plasma frequency, which finally lead to the emission of one attosecond light pulse per laser cycle. Clear criteria are known for the discrimination of the two types of SHHG emission.

(i) Spectral extent: CWE emission extends no further than the maximum plasma frequency given by the solid-target density, which corresponds to a cutoff-photon-energy of $\approx 30\,\mathrm{eV}$ for an SiO_2 target. In contrast, for sufficiently high driving intensities, relativistic SHHG can extend well beyond this CWE cutoff.

(ii) Intensity dependence: CWE is a linear process, i.e. the laser-to-SHHG conversion efficiency of CWE is constant over a large driving intensity range $> 10^{15}\,\mathrm{W/cm^2}$ [1], whereas relativistic SHHG is highly nonlinear, i.e. the conversion efficiency increases rapidly over a large a_0-range from $a_0 \sim 1$ until a saturation in the the ultra-relativistic limit $a_0 \sim 100$ [1, 20]. Note however that in the experimentally still well out-of-reach ultra-relativsitic regime, the radiation reaction force may significantly modify SHHG [23].

(iii) Phase properties: The intensity-dependence of the Brunel trajectories leads to increasing delays between successive attosecond pulses during the driving pulse envelope, and thus to frequency-broadened negatively chirped individual harmonics [21, 24]. A positively chirped driving pulse can partially compensate the effect and consequently lead to spectrally narrower CWE-harmonics [21, 25]. In contrast, for moderately relativsitic $a_0 \sim 1$, the relativsitic SHHG emission is Fourier-limited [1] such that despite its much steeper intensity dependence and consequently shorter temporal envelope, its harmonic spectral width is narrower than that of CWE harmonics generated in the same conditions [1, 9, 26]. Only for higher $a_0 \gtrsim 10$, plasma surface denting due to radiation pressure will again induce an intrinsic harmonic chirp, with the opposite sign compared to that of CWE [1, 27].

(iv) Dependence on the plasma density gradient: In CWE, the electron density peak formation and conversion of plasma oscillations to light are both optimized for rather steep plasma density gradients. The optimal scale length is $Ł \sim \lambda_0/100$ for higher-order CWE harmonics, followed by a rapid drop for increasing Ł [1]. Furthermore, the intrinsic harmonic chirp and thus the spectral width of CWE-harmonic peaks increases with Ł [21, 25]. In contrast, the optimal Ł for relativistic SHHG is longer and has been consistently found in single-shot experiments near a scale length $Ł \approx \lambda_0/10$ [4, 5, 26, 28]. This can be shown to be consistent with particle-in-cell simulations, which often treat initially step-like plasma density profiles with variable peak density n. This adjusts the similarity parameter $S = n/(n_c a_0)$, which scales laser plasma-interaction in the relativistic regime [29]. The optimal conditions for the relativistic push-pull process, relying on the formation and dynamics of a sharp and high electron density spike, are predicted for $S \approx 1$ to 5, i.e. a few times overdense plasmas [15, 16, 20]. In the experimentally relevant case for solid targets of a smooth surface plasma density profile rising up to $\sim 100 n_c$ bulk density, one may define an effective S_{eff}, as demonstrated in ref. [30] for a linear density ramp.

Considering instead the exponential density profile $n(x)$ defined in the introduction, the balance of the laser's Lorentz force and the electrostatic restoring force exerted by the plasma ion background [14, 27] yields a position of the electron density spike, averaged over the "pushing cycle" of the laser field, of $x_{\mathrm{b}} = Ł \ln\{[a_0(1+\sin\theta)\cos\theta]/[2\pi(Ł/\lambda_0)]\}$, where θ is the laser incidence angle on the plasma surface. Experimentally varying the plasma density gradient scale length Ł thus corresponds to adjusting the effective plasma (ion) density $n[x_{\mathrm{b}}(Ł)]$. This yields an effective similarity parameter $S_{\mathrm{eff}} = n(x_{\mathrm{b}})/(n_c a_0) = (1+\sin\theta)\cos\theta/[2\pi(Ł/\lambda_0)]$. The range $S_{\mathrm{eff}} \in [1,5]$ is thus achieved for $Ł \in [\lambda_0/30, \lambda_0/6]$, independently of the

laser peak intensity. This is perfectly consistent with the existing experimental results as well as with those we report in this letter. Finally, for longer Ł, SHHG disappears due to the onset of chaotic electron dynamics in the long low-density [4].

(v) Simultaneous electron emission: The same optimal Ł $\approx \lambda_0/10$ has been found for the emission of high-energy electrons from a plasma mirror [31], which is therefore found to be correlated to relativistic SHHG [4] and be anti-correlated to CWE [32].

The experiment was carried out using the 1-kHz Salle Noire laser system at LOA, delivering pulses with durations adjustable between 24 and < 4 fs and temporal contrast ($> 10^{10}$) [11]. For SHHG, the p-polarized pulses are focused by an f/1.5, 30° off-axis parabola onto a rotating optically flat fused silica target at an incidence angle of $\theta = 55°$ to an $\approx$ 1.8-µm FWHM spot. With a pulse energy of 2.6 mJ on target, this yields, supposing absence of spatio-temporal distortions, peak intensities of 2.5×10^{18} W/cm^2 ($a_0 = 1.1$ for $\lambda_0 = 800$ nm), 7×10^{18} W/cm^2 ($a_0 = 1.8$ for $\lambda_0 = 800$ nm), and 1.0×10^{19} W/cm^2 ($a_0 = 2.0$ for $\lambda_0 = 720$ nm) for 24-fs, 9-fs and 4-fs pulses, respectively. We thus operate in an intensity regime where both CWE and relativsitic SHHG can be expected to give significant contributions to the generated harmonic signal. A spatially superposed pre-pulse, created by picking off and then recombining $\approx 4\%$ of the main pulse through holey mirrors, is focused to a much larger 13 µm FWHM spot in order to generate a homogeneous plasma expanding into vacuum. A pre-pulse lead time τ of a few ps lets us density gradient scale length Ł $= L_0 + c_s\tau$. The expansion speed c_s is measured with spatial-domain interferometry (SDI) [33] and L_0 is the scale length increase owing to the limited temporal contrast of the main pulse. The fact that we do observe CWE emission (see below) justifies the assumptions that $L_0 \lesssim \lambda_0/50$.

The emitted SHHG radiation in the specular direction is recorded using an angularly resolving XUV spectrometer, including a gold-coated flat-field grating (600 lines/mm, 85.3° incidence) and micro-channel-plate (MCP) and phosphor screen detector. The MCP is time-gated for ≈ 250 ns synchronously with the laser pulses so as to suppress longer background plasma emission. The phosphor screen is finally imaged by a charged-coupled-device (CCD) camera to record angularly resolved ($[-30, 30]$ mrad) SHHG spectra. This only detects the central part of the the emitted SHHG beam, which in our conditions, owing in particular to the small source spot, has a FWHM-divergence of $\gtrsim 70$ mrad. The SHHG-spectra shown in the follwoing are angularly integrated over the full range and represent the MCP signal without corretion for the spectral response of the XUV spectrometer so as to enhance the visibility of the higher harmonic orders.

Synchronuously, we detect the angular emission profile of electrons with energies > 150keV with a lanex-screen [34], placed between the specular and the target-normal directions imaged by another CCD camera. The distributions along the azimuthal angle (in the incidence plane) shown in the following are integrated over the polar angle (perpendicualr to the incidence plane).

All data shown are acquired by integrating over 100-ms long bursts of pulses at 1 kHz repetition rate, i.e. over 100 shots.

Figure 1(a) shows results obtained with a near-Fourier-limited 24-fs driver pulse. The pre-pulse lead time is scanned between 0 and 10 ps. Via an SDI measurement, this translates to a change of plasma density gradient scale length from L_0 to $L_0 + \lambda_0/10$, where $\lambda_0 = 800$nm. Two Ł-regimes are clearly distinguished. At the shortes gradients Ł $- L_0 > \lambda_0/50$, the harmonic peaks are broad and their intensity quickly drops with increasing Ł, as expetected for CWE emission. At higher Ł, the harmonic peaks are remarkably narrower and their intensity goes through an optimum located at Ł $- L_0 \approx 0.06\lambda_0$, consistent with the theoretical expectations for relativistic SHHG emission as well as with earlier experimental observation with similar multi-cycle driver pulses [4, 5, 26, 28]. We also remark that no harmonics are visible beyond the CWE-cutoff at 30 eV, even for softer gradients. This is not very surprising as the laser intensity is only just around the relativistic threshold, $a_0 = 1.1$. Finally, we find a stronger electron emission at softer gradients, correlated to the (presumed) relativistic SHHG emission.

We can corroborate this interpretation by using a "Dazzler" acousto-optic programmable dispersive filter in our amplifier chain to add 500 fs^2 GDD to the driving pulses, thus chirping them positively, stretching them to 85 fs duration and consequently decreasing the intensity to 0.7×10^{18} W/cm^2 ($a_0 = 0.6$ for $\lambda_0 = 800$ nm). As

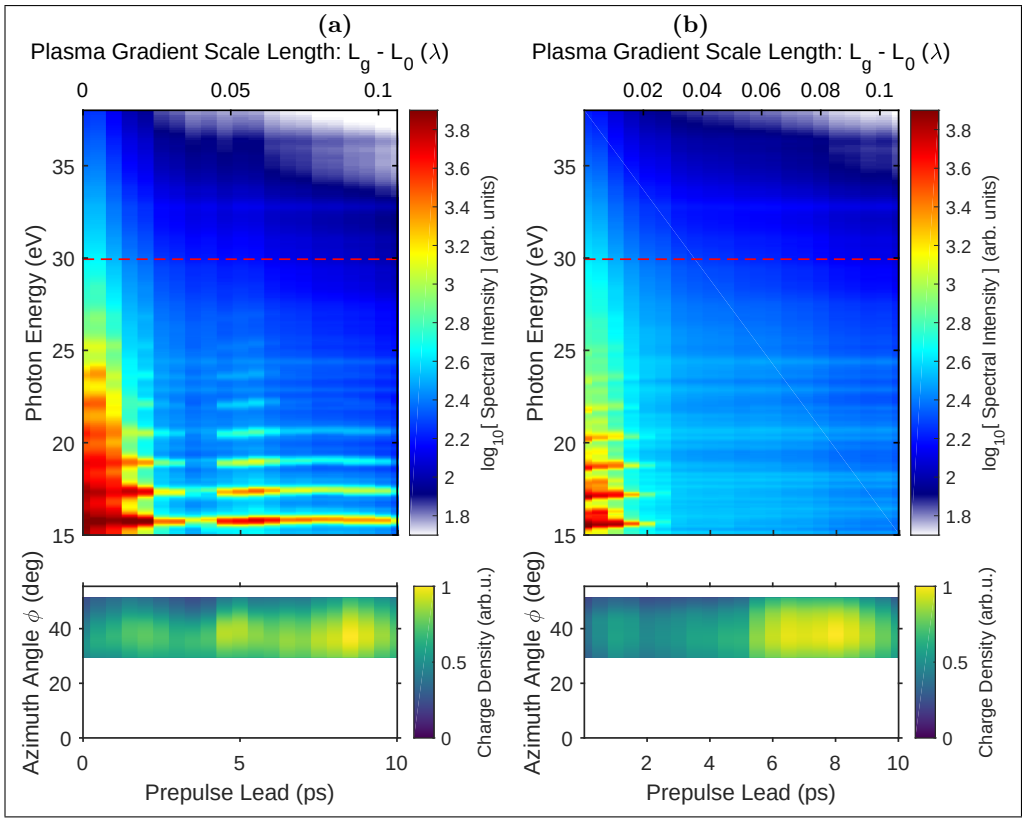


FIG. 1. Synchronously measured SHHG (upper, log-scale) and electron (lower) emission as a function of the plasma gradient scale length. The dashed red line marks the CWE cutoff energy. The normal and specular directions correspond to $\phi = 0$ and $\phi = 55°$. (a) For a compressed, 24-fs, $a_0 = 1.1$ driver pulse, (b) for the same pulse with added 500 fs^2 GDD, 85 fs duration, $a_0 = 0.6$.

shown in figure 1(b), the harmonic spectral widths reduce significantly at the shortest Ł, but remain at similar intensity. This is consistent with the compensation of the aperiodicity of the CWE attosecond pulse train and the linearity of the CWE process. The SHHG emision at softer gradients however disappears completely, consistent with a highly nonlinear intensity-dependence of relativistic SHHG. Electrons are still emitted preferentially for the softer gradients and the resulting anti-correlation of harmonics and electrons is reminiscent of our earlier sub-relativistic-intensity results reported in ref. [32].

Reducing the driving pulse duration to 9 fs at constant pulse energy increases the peak normalized vector potential to $a_0 = 1.8$ and leads to the results shown in Figure 2. The same features as for the 24-fs driver can be observed, i.e. a transition from spectrally broad harmonics at the shortest Ł towards a "cleaner" well-modulated harmonic spectrum around an optimal Ł $- L_0 \approx 0.06\lambda_0$, and a correlation of the relativistic SHHG with electron emission for softer gradients. Additionally, we now observe a spectral extent of the SHHG signal slightly beyond the CWE-cutoff, which is definite proof for relativistic SHHG, reported here for the first time with a 1-kHz repetition rate. For longer Ł, the relativistic SHHG signal persists until at least Ł $= \lambda/5$ but their intensity and spectral extent gradually descreases.

An even shorter 4-fs driving pulse may be expected to strongly boost the SHHG signal beyond the CWE cutoff. Self-steepening in the helium-filled hollow-core fiber used for post-compression however reduces the central wavelength to $\lambda_0 = 720$nm [11] so that despite a constant on-target pusle energy, the peak normalized vector potential only incresease to $a_0 = 2.0$. Furthermore, such short pulses become extremely sensitive to spatio-temporal couplings which can drastically reduce the achievable peak intensity. On many days we thus observe reduced spectral extent of the SHHG spectra generated with $\lesssim$ 4-fs pulses as compared to those obtained with 9-fs pulses shown in Fig. 2, as was the case for the experiments reported in ref. [35].

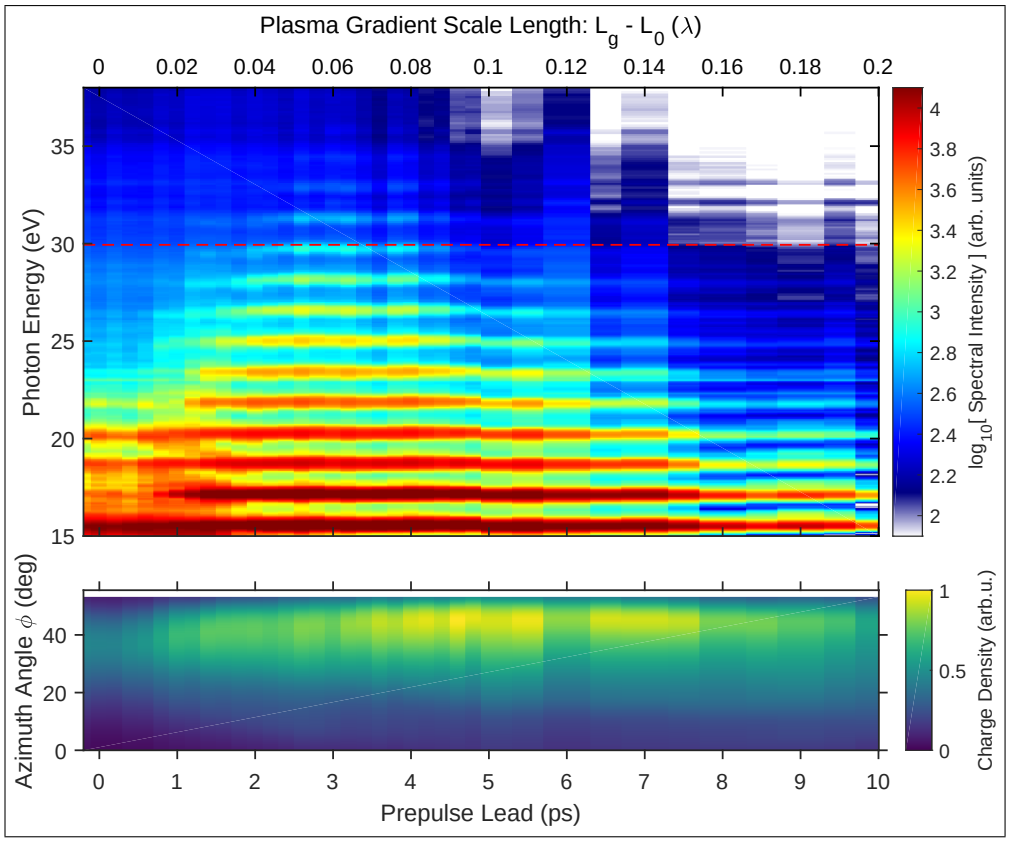


FIG. 2. Synchronously measured SHHG (upper, log-scale) and electron (lower) emission as a function of the plasma gradient scale length for a 9-fs, $a_0 = 1.8$ driver pulse. The dashed red line marks the CWE cutoff energy. The normal and specular directions correspond to $\phi = 0$ and $\phi = 55°$.

We did nonetheless suceed in recording the dataset shown in Figure 3 with a 4-fs driving pulse and shot-to-shot randomly varying carrier-envelope phase. As for the 9-fs result, relativsitic SHHG is optimized for plasma density gradient scale lengths between Ł $- L_0 \approx \lambda/25$ and $\lambda/10$, where $\lambda = 800$ nm, consistent with the theoretical prediction. The optimal relativsitic SHHG spectra now extend well beyond the CWE cutoff. The spectra still present a discernible harmonic modulation, in particular for the softer gradients, and one can make out small gradual Ł-dependent shifts of the harmonic peaks. These may result from a varying temporal structure of the generated very short attsecond pulse-train. While all recorded spectra are continua, i.e. the harmonic peaks spectrally overlap, the absence of CEP-stability however precludes any further discussion of this temporal structure [35].

In conclusion, we have reported clear evidence for the first generation of XUV spectra from relativistic SHHG on plasma mirrors at a kilohertz repetition rate, emitted simultaneously and correlated to the emission of energetic electrons. We have presented and discussed measurements of SHHG spectra and electron angular distributions as a function of the experimentally controlled plasma density gradient scale length Ł for three increasingly short and intense driving pulses: 24 fs (9 optical cycles) and $a_0 = 1.1$, 9 fs (3.5 optical cycles) and $a_0 = 1.8$, and finally 4 fs (1.7 optical cycles) and $a_0 \approx 2.0$. For all driver pulses, we observe relativistic SHHG in the range Ł $\in [\lambda/25, \lambda/10]$, with an optimum gradient scale length of Ł $\approx \lambda/15$.

These results open the route to detailed a examination and optimization of relativistic SHHG exploiting the high kHz-repetition rate and exceptional stability of our laser system. In particular for the shortest driver durations and with added CEP-locking, we should become able to harness the favorable phase properties of relativsitic SHHG for the generation of powerful isolated attosecond pulses from plasma mirrors [35].

Funding. Agence Nationale pour la Recherche (ANR-11-EQPX-005-ATTOLAB, ANR-14-CE32-0011-03 APERO); Investissements dAvenir program LabEx PALM

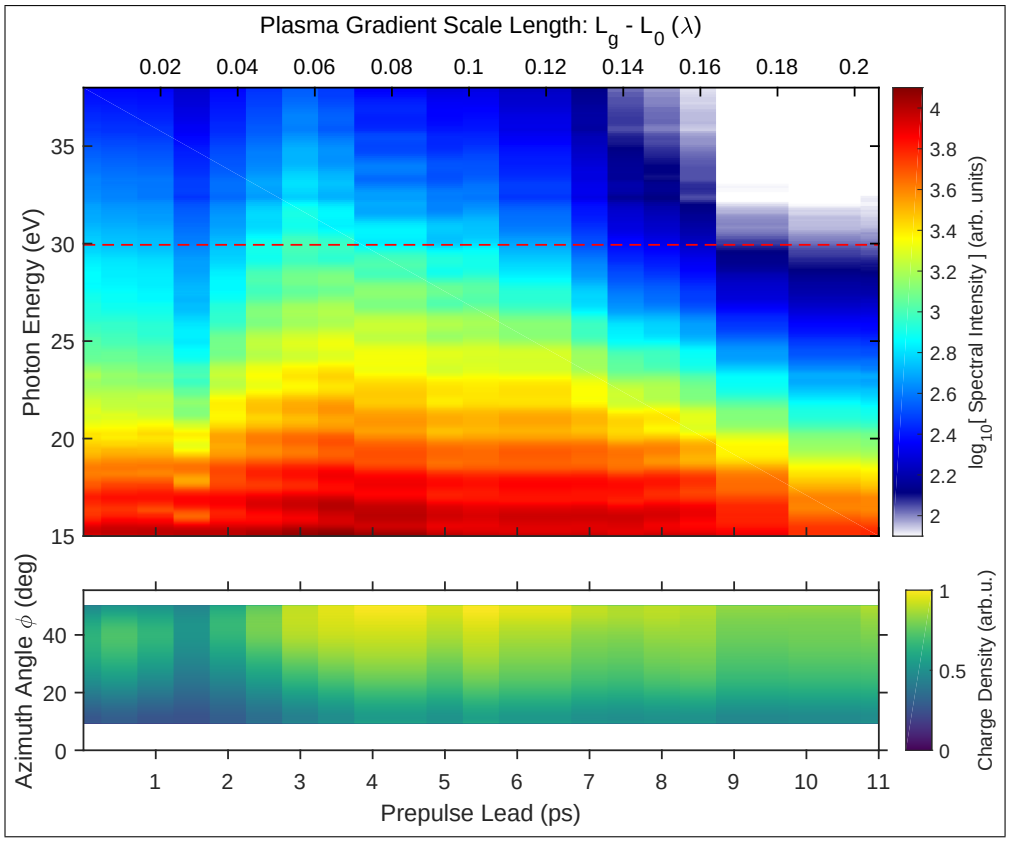


FIG. 3. Synchronously measured SHHG (upper, log-scale) and electron (lower) emission as a function of the plasma gradient scale length for a 4-fs, $a_0 = 2.0$ driver pulse. The dashed red line marks the CWE cutoff energy. The normal and specular directions correspond to $\phi = 0$ and $\phi = 55°$.

(ANR-10-LABX-0039-PALM); European Research Council (ERC FEMTOELEC 306708, ERC ExCoMet 694596); LASERLAB-EUROPE (H2020-EU.1.4.1.2. grant agreement ID 654148), Région Ile-de-France (SESAME 2012-ATTOLITE).

[1] C. Thaury and F. Qur, High-order harmonic and attosecond pulse generation on plasma mirrors: basic mechanisms, Journal of Physics B: Atomic, Molecular and Optical Physics **43**, 213001 (2010).

[2] G. D. Tsakiris, K. Eidmann, J. Meyer-ter Vehn, and F. Krausz, Route to intense single attosecond pulses, New Journal of Physics **8**, 19 (2006).

[3] an der Brügge and A. Pukhov, Enhanced relativistic harmonics by electron nanobunching, Physics of Plasmas **17**, 033110 (2010).

[4] L. Chopineau, A. Leblanc, G. Blaclard, A. Denoeud, M. Thvenet, J.-L. Vay, G. Bonnaud, P. Martin, H. Vincenti, and F. Qur, Identification of Coupling Mechanisms between Ultraintense Laser Light and Dense Plasmas, Physical Review X **9**, 011050 (2019).

[5] C. Rödel, an der Brügge, J. Bierbach, M. Yeung, T. Hahn, B. Dromey, S. Herzer, S. Fuchs, A. G. Pour, E. Eckner, M. Behmke, M. Cerchez, O. Jäckel, D. Hemmers, T. Toncian, M. C. Kaluza, A. Belyanin, G. Pretzler, O. Willi, A. Pukhov, M. Zepf, and G. G. Paulus, Harmonic generation from relativistic plasma surfaces in ultrasteep plasma density gradients, Phys. Rev. Lett. **109**, 125002 (2012).

[6] P. Heissler, A. Barna, J. M. Mikhailova, G. Ma, K. Khrennikov, S. Karsch, L. Veisz, I. B. Földes, and G. D. Tsakiris, Multi-μJ harmonic emission energy from laser-driven plasma, Applied Physics B , 1 (2014).

[7] M. Yeung, S. Rykovanov, J. Bierbach, L. Li, E. Eckner, S. Kuschel, A. Woldegeorgis, C. Rdel, A. Svert, G. G. Paulus, M. Coughlan, B. Dromey, and M. Zepf, Experimental observation of attosecond control over relativistic electron bunches with two-colour fields, Nature Photonics **11**, 32 (2017).

[8] O. Jahn, V. E. Leshchenko, P. Tzallas, A. Kessel, M. Krger, A. Mnzer, S. A. Trushin, G. D. Tsakiris, S. Kahaly, D. Kormin, L. Veisz, V. Pervak, F. Krausz, Z. Major, and S. Karsch, Towards intense isolated attosecond pulses from relativistic surface high harmonics, Optica **6**, 280 (2019).

[9] C. Thaury, F. Qur, J. P. Geindre, A. Levy, T. Ceccotti, P. Monot, M. Bougeard, F. Reau, P. d/'Oliveira, P. Audebert, R. Marjoribanks, and P. Martin, Plasma mirrors for ultrahigh-intensity optics, Nature Physics **3**, 424 (2007).

[10] A. Jullien, O. Albert, F. Burgy, G. Hamoniaux, J.-P. Rousseau, J.-P. Chambaret, F. Aug-Rochereau, G. Chriaux, J. Etchepare, N. Minkovski, and S. M. Saltiel, 10^{-10} temporal contrast for femtosecond ultraintense lasers by cross-polarized wave generation, Opt. Lett. **30**, 920 (2005).

[11] M. Ouill, A. Vernier, F. Bhle, M. Bocoum, A. Jullien, M. Lozano, J.-P. Rousseau, Z. Cheng, D. Gustas, A. Blumenstein, P. Simon, S. Haessler, J. Faure, T. Nagy, and R. Lopez-Martens, Relativistic-intensity near-single-cycle light waveforms at khz repetition rate, Light: Science & Applications **9**, 1 (2020).

[12] D. Gunot, D. Gustas, A. Vernier, B. Beaurepaire, F. Bhle, M. Bocoum, M. Lozano, A. Jullien, R. Lopez-Martens, A. Lifschitz, and J. Faure, Relativistic electron beams driven by kHz single-cycle light pulses, Nature Photonics **11**, 293 (2017).

[13] N. Zam, F. Bhle, M. Bocoum, A. Vernier, S. Haessler, X. Davoine, L. Videau, J. Faure, and R. Lopez-Martens, Few-cycle laser wakefield acceleration on solid targets with controlled plasma scale length, Physics of Plasmas **26**, 033112 (2019).

[14] M. Thvenet, H. Vincenti, and J. Faure, On the physics of electron ejection from laser-irradiated overdense plasmas, Physics of Plasmas **23**, 063119 (2016).

[15] A. A. Gonoskov, A. V. Korzhimanov, A. V. Kim, M. Marklund, and A. M. Sergeev, Ultrarelativistic nanoplasmonics as a route towards extreme-intensity attosecond pulses, Physical Review E **84**, 046403 (2011).

[16] A. Gonoskov, Theory of relativistic radiation reflection from plasmas, Physics of Plasmas **25**, 013108 (2018).

[17] R. Lichters, M. t. Vehn, and A. Pukhov, Short-pulse laser harmonics from oscillating plasma surfaces driven at relativistic intensity, Physics of Plasmas **3**, 3425 (1996).

[18] S. Gordienko, A. Pukhov, O. Shorokhov, and T. Baeva, Relativistic Doppler Effect: Universal Spectra and Zeptosecond Pulses, Physical Review Letters **93**, 115002 (2004).

[19] J. M. Mikhailova, M. V. Fedorov, N. Karpowicz, P. Gibbon, V. T. Platonenko, A. M. Zheltikov, and F. Krausz, Isolated Attosecond Pulses from Laser-Driven Synchrotron Radiation, Physical Review Letters **109**, 245005 (2012).

[20] M. R. Edwards and J. M. Mikhailova, The X-Ray Emission Effectiveness of Plasma Mirrors: Reexamining Power-Law Scaling for Relativistic High-Order Harmonic Generation, Scientific Reports **10**, 1 (2020).

[21] F. Qur, C. Thaury, P. Monot, S. Dobosz, Martin, Ph., J. P. Geindre, and P. Audebert, Coherent Wake Emission of High-Order Harmonics from Overdense Plasmas, Physical Review Letters **96**, 125004 (2006).

[22] F. Brunel, Not-so-resonant, resonant absorption, Physical Review Letters **59**, 52 (1987).

[23] S. Tang, N. Kumar, and C. H. Keitel, Plasma high-order-harmonic generation from ultraintense laser pulses, Physical Review E **95**, 051201 (2017).

[24] K. Varj, Y. Mairesse, B. Carr, M. B. Gaarde, P. Johnsson, S. Kazamias, R. Lopez-Martens, J. Mauritsson, K. J. Schafer, P. Balcou, A. L'Huillier, and P. Salires, Frequency chirp of harmonic and attosecond pulses, Journal of Modern Optics **52**, 379 (2005).

[25] A. Malvache, A. Borot, F. Qur, and R. L. Martens, Coherent wake emission spectroscopy as a probe of steep plasma density profiles, Physical Review E **87**, 035101 (2013).

[26] S. Kahaly, S. Monchoc, H. Vincenti, T. Dzelzainis, B. Dromey, M. Zepf, P. Martin, and F. Qur, Direct Observation of Density-Gradient Effects in Harmonic Generation from Plasma Mirrors, Physical Review Letters **110**, 175001 (2013).

[27] H. Vincenti, S. Monchoc, S. Kahaly, G. Bonnaud, P. Martin, and F. Qur, Optical properties of relativistic plasma mirrors, Nature Communications **5**, 3403 (2014).

[28] J. Gao, B. Li, F. Liu, H. Cai, M. Chen, X. Yuan, X. Ge, L. Chen, Z. Sheng, and J. Zhang, Double optimal density gradients for harmonic generation from relativistically oscillating plasma surfaces, Physics of Plasmas **26**, 103102 (2019).

[29] S. Gordienko and A. Pukhov, Scalings for ultrarelativistic laser plasmas and quasimonoenergetic electrons, Physics of Plasmas **12**, 043109 (2005).

[30] T. G. Blackburn, A. A. Gonoskov, and M. Marklund, Relativistically intense XUV radiation from laser-illuminated near-critical plasmas, Physical Review A **98**, 023421 (2018).

[31] M. Thvenet, A. Leblanc, S. Kahaly, H. Vincenti, A. Vernier, F. Qur, and J. Faure, Vacuum laser acceleration of relativistic electrons using plasma mirror injectors, Nature Physics **12**, 355 (2016).

[32] M. Bocoum, M. Thvenet, F. Bhle, B. Beaurepaire, A. Vernier, A. Jullien, J. Faure,

and R. Lopez-Martens, Anticorrelated Emission of High Harmonics and Fast Electron Beams From Plasma Mirrors, Physical Review Letters **116**, 185001 (2016).

[33] M. Bocoum, F. Bhle, A. Vernier, A. Jullien, J. Faure, and R. Lopez-Martens, Spatial-domain interferometer for measuring plasma mirror expansion, Optics Letters **40**, 3009 (2015).

[34] Y. Glinec, J. Faure, A. Guemnie-Tafo, V. Malka, H. Monard, J. P. Larbre, V. De Waele, J. L. Marignier, and M. Mostafavi, Absolute calibration for a broad range single shot electron spectrometer, Review of Scientific Instruments **77**, 103301 (2006).

[35] F. Bhle, M. Thvenet, M. Bocoum, A. Vernier, S. Haessler, and R. Lopez-Martens, Generation of XUV spectral continua from relativistic plasma mirrors driven in the near-single-cycle limit, arXiv:2003.04688 [physics] (2020), arXiv: 2003.04688.